LA-UR-79-168

TITLE: CROSS-SECTION SENSITIVITY AND UNCERTAINTY ANALYSIS FOR FUSION REACTORS (A REVIEW)

AUTHOR(S): Donald J. Dudziak

SUBMITTED TO: IAEA Advisory Group Meeting
Nuclear Data for Fusion Reactor Technology
Vienna, Austria
December 11-15, 1978

los alamos
scientific laboratory
of the University of California
LOS ALAMOS, NEW MEXICO 87544

An Affirmative Action/Equal Opportunity Employer

Form No. 836
St. No. 2629
1/75

UNITED STATES
ENERGY RESEARCH AND
DEVELOPMENT ADMINISTRATION
CONTRACT W-7405-ENG-36

CROSS-SECTION SENSITIVITY AND UNCERTAINTY ANALYSIS FOR FUSION REACTORS (A REVIEW)*

Donald J. Dudziak
Theoretical Division
University of California
Los Alamos Scientific Laboratory
Los Alamos, New Mexico, USA

ABSTRACT

A review is presented of neutron cross-section sensitivity and uncertainty studies as applied to fusion reactor concepts. General observations are made concerning the applicability and potential value of such studies, as well as their current limitations. While literature is cited relative to sensitivities to D-D and D-T cross sections, as well as to temperature of the D-T reaction, these topics are excluded from discussion. After a brief review of cross-section and secondary-energy-distribution sensitivity theory, most emphasis is focused upon published studies of the TFTR, experimental power reactors, and a conceptual commercial reactor (NOMAD). Salient results of these studies, as they pertain to cross-section measurement and evaluation requirements, are summarized. Lastly, some comments are made relative to cross-section data requirements in the 14-50 MeV region.

---

*Work performed under the auspices of the U. S. Department of Energy.

I. INTRODUCTION

Under the topic of sensitivity and uncertainty analysis we consider primarily the work performed using classical perturbation theory and cross-section uncertainty covariance data. Specifically excluded are several studies performed using alternate evaluated data sets or credibly deviant data sets devised by the analyst. Fusion reactor nucleonics analysis being a comparatively new field of endeavor, the scope of this review is thus confined to relatively few papers, mainly those reporting cross-section sensitivity* studies of the Tokamak Fusion Test Reactor (TFTR) and experimental power reactor (EPR) design studies. In order to keep the topic more manageable, we also exclude any detailed discussion of hybrid reactor sensitivity studies. However, this does not imply a lack of recognition of the importance of hybrid reactor concepts or of the vital role cross-section data play in conceptual hybrid design exercises. Rather, it reflects a lack of published investigations in this area, with two notable exceptions.[1a,1b] Likewise, application of sensitivitity methods to design and analysis of integral experiments, although very important is beyond our scope.

Upon the recommendation of the International Nuclear Data Committee, data up to 50 MeV are included in this review. However, no uncertainty studies per se have been performed for neutron energies above ~ 14 MeV, so review comments are necessarily mostly qualitative.

Other areas where sensitivity studies exist in the literature, but which are specifically excluded from this review, are the sensitivity of multigroup cross section to thermal broadening of the fusion peak,[2] and of plasma burn to the D-D and D-T cross sections.[3]

The theory of cross-section sensitivity is fortuitously simpler for fusion reactors than for fission reactors, because eigenvalue problems are obviated. Most analyses involve only inhomogeneous source terms in the linear Boltzmann equation, leading to a relatively simple logarithmic derivative of a reaction rate with respect to a cross-section. In Sec. II below a brief summary of the theory is given, including recent extensions to secondary energy and angular distributions.[4,5] Section III then presents a discussion of detailed results from the literature, for the TFTR, EPR, and a conceptual commercial power reactor (NUWMAK). Also, comments are made in Sec. III regarding data in the region above 14 MeV. Conclusions from the studies in Sec. III are then summarized in Sec. IV.

At the outset it is useful to make a salient, if perhaps obvious, point regarding sensitivity studies. That is, such studies are intrinsically design dependent, as is explicitly shown in the theory (Sec. II). The immediate implication is that the question, "Are the available cross-section data for a particular nuclide 'N' satisfactory for fusion reactor design?" is unfinished, leaving wanting two key qualifiers; viz, 1) for what design model, and 2) for which response functions. Another clear observation is that sensitivity studies are analogous to cross-section assessments done previously by cruder methods for fission and fusion devices, albeit more comprehensive and providing differentials of uncertainty rather than just point values. Being design-dependent does not, however, mean that broader conclusions than those for a specific design cannot be drawn from a sensitivity analysis. On the contrary, for a generic class of designs the sensitivity results for a prototypic set of design models can span the range of sensitivities for that class. A practical case in point is the sensitivity analysis[6] performed for an EPR design, where the conclusions drawn may be largely valid for a later design study of a reactor concept called The Next Step (TNS).

Another facet of sensitivity studies which may be self-evident is that they are of direct value to both the reactor designer and the cross-section technologist.

---

*In this review we will use the abbreviated phrase "sensitivity" studies to include uncertainty analyses where it is clear from the context.

Their immediate value to the designer is to furnish him requirements for a margin-of-safety component attributable to nucleonic uncertainties, which he can then factor into design conservatisms. Secondly, the sensitivities can guide him in selection of materials and configurations which will perhaps minimize nucleonic uncertainties while still satisfying design criteria (e.g., selection of shielding materials). Concurrently, the cross-section technologist is able to determine which additional experiments and/or evaluations are most likely to, first, significantly decrease uncertainties, and, second, yield the lowest cost-benefit ratio. While the foregoing qualitative introductory discussion deals with a somewhat idealized application, many of the benefits mentioned have already been realized. One case in point is the TFTR, where the value of the sensitivity analysis manifested itself in the "negative" result that anticipated cross-section errors should not be unacceptable for calculations of radiation exposure rate during required access after reactor shutdown.

Historically, the modern development of sensitivity and uncertainty analysis can be traced from the work of Prezbindowski[7] in 1968, to a mushrooming expansion and application by Conn,[8] Bartine,[9,10] Gerstl,[11,12] and their respective colleagues in the early 1970's. Some of these early applications were already to fusion reactors.[8,9,12,13,14] The total fusion reactor sensitivity literature, however, is still somewhat limited because of the relative newness of fusion reactor nucleonics. It is still possible for a serious practitioner interested in nuclear analysis or cross-section technology to readily familiarize himself with most of these publications (e.g., Refs. 1, 4, 6, 8, 9, 12-19). More basic literature on the theoretical foundations of sensitivity theory can be found among the references given in Refs. 8 and 19.

With the notable exception of secondary energy and angular distribution sensitivity, sensitivity studies have been hindered not primarily by theoretical methods or computer code availability, but rather by lack of cross-section covariance data. Strictly sensitivity (not including uncertainty) analyses are readily performed using standard discrete-ordinates transport codes and subsequent straightforward integrations over the Boltzmann equation phase space. However, the uncertainty analysis then requires covariance data which can be equally voluminous as the cross-section data entering the purely sensitivity analysis. In practice, evaluated covariance data have only recently become available in the ENDF, and those are still preliminary and sparse. Hence, most uncertainty analyses to date have by necessity used ad-hoc covariance data, most of which contain no covariances among partial cross-sections. From the outset it is clear that the surface has just been scratched in uncertainty analysis and, to extend the metaphor, the cutting edge is now the covariance evaluation efforts.

II. SENSITIVITY AND UNCERTAINTY THEORY

Cross-section sensitivity theory has been derived by various authors from several points of view. Here the approaches of Refs. 10, 18, and 19 are eclectically synthesized for an exposition ending with a transparent parallelism to the actual computational procedure. Secondary energy and angular distribution sensitivity theory discussions follow the approach of Refs. 4 and 5.

A. Cross Sections

Given a cross-section uncertainty, $\Delta\Sigma$, the objective is to determine the uncertainty, ΔR, in a selected response, R, where R is a linear functional of the flux $\phi(\xi)$. In general, we will deal with the phase space of the Boltzmann equation,

$$\vec{\xi} = (\vec{r},\vec{\Omega},E) \qquad (1)$$

in the conventional notation.

Concentrating on a set of multigroup cross-section data $\{\Sigma_i\}$, we seek an expression for the standard deviation of R, which we denote ΔR, in terms of the known covariances of the $\{\Sigma_i\}$. First, we note that R is defined by

$$R = \langle \phi, \rho \rangle \ , \tag{2}$$

where ρ is a given response function, and the inner-product notation $\langle , \rangle$ represents integration over the phase space ξ. Also, the forward and adjoint Boltzmann equations can be written conveniently in operator notation as

$$L\phi = S \tag{3}$$

$$L^*\phi^* = \rho \ , \tag{4}$$

where L and L* are the respective transport operators, S is the inhomogeneous source term, and $\rho(\xi)$ is the response function of interest (i.e., the adjoint source). Then from well-known variational principles it can be shown that for $R = \langle \psi, \rho \rangle = \langle \phi, L^*\psi^* \rangle$,

$$\delta R = \langle \phi, \delta\rho \rangle - \langle \phi, \delta L^* \phi^* \rangle + 0^2 \ . \tag{5}$$

Then if L_i is the portion of the operator containing Σ_i, by the linearity of L we can write[10,18]

$$\frac{\partial R/R}{\partial \Sigma_i / \Sigma_i} = \frac{\langle \phi, \rho \rangle_i}{R} - \frac{\langle \phi, L_i^* \psi^* \rangle_i}{R} \ , \tag{6}$$

where the first term on the right is a direct effect of a change in the response function, and is nonzero only if the response function depends directly on Σ_i (e.g., if ρ is a linear function of Σ_i). In practice the two terms are treated separately because only the second term involves any complexity. Note that Eq. (6) involves integration over all phase space, except the variable E when i denotes an energy group. By convention the energy variable is usually kept explicit and a differential (with respect to lethargy) *sensitivity profile* is defined as follows:

$$P'_{\Sigma_i} \triangleq - \frac{\partial(\ell n R)}{\partial(\ell n \Sigma_i) d(\ell n E)} = \frac{\partial R/R}{\frac{\partial \Sigma_i}{\Sigma_i} du} \ , \tag{7}$$

or

$$P'_{\Sigma_i} \triangleq - \frac{\langle \phi, L_i^* \phi^* \rangle_i}{R \Delta u_i} \tag{8}$$

when i denotes an energy group of lethargy width Δu_i. An important point to keep in mind, however, is that in the theory leading to Eq. (6), the subscript i can denote any partition of the transport operator (e.g., into partial cross-sections), not just an energy-group partition. Thus, P_{Σ_i} has a supressed index which in normal practice represents the partial cross-section, while i represents an energy group. Further, the domain of phase space is often subdivided so as to determine

sensitivity profiles for individual material zones, for example. In fact, the definition of a sensitivity profile as in Eq. (8) can follow naturally from a differential sensitivity profile given by

$$P_{\Sigma_i}(\vec{\xi}) = -\frac{\partial(\ell nR)}{\partial(\ell n\Sigma_i)d\vec{\xi}} = \frac{\phi L_i^* \phi^*}{R} \quad . \tag{9}$$

Returning now to the calculation of ΔR, which is defined as the positive square root

$$\Delta R \equiv [E\{\delta R^2\}]^{1/2} \equiv [Var(R)]^{1/2} \quad , \tag{10}$$

where $E\{\}$ denotes an expectation value, we formally can write

$$Var(R) = E\left\{ \sum_{i,j} \frac{\partial R}{\partial \Sigma_i} \delta\Sigma_i \frac{\partial R}{\partial \Sigma_j} \delta\Sigma_j \right\} \quad , \tag{11}$$

where we accept the assumptions of linear perturbation theory; i.e.,

$$\delta R = \sum_i \frac{\partial R}{\partial \Sigma_i} \delta\Sigma_i \quad . \tag{12}$$

Equation (11) can then be written

$$Var(R) = \sum_{i,j} \frac{\partial R}{\partial \Sigma_i} \frac{\partial R}{\partial \Sigma_j} E\{\delta\Sigma_i \delta\Sigma_j\} \quad , \tag{13}$$

where $E\{\delta\Sigma_i \delta\Sigma_j\}$ is commonly called the covariance or dispersion matrix for the set $\{\Sigma_i\}$. Dividing Eq. (13) by R^2 yields

$$\left(\frac{\Delta R}{R}\right)^2 = \sum_{i,j} P_{\Sigma_i} P_{\Sigma_j} \left[\frac{Cov(\Sigma_i, \Sigma_j)}{\Sigma_i \Sigma_j}\right], \tag{14}$$

where $P_{\Sigma_i} = \Delta u_i P'_{\Sigma_i}$. For compactness we define a sensitivity profile vector

$$\underline{P} = [P_{\Sigma_i}] \tag{15}$$

and a relative covariance matrix

$$\underline{C} = \left[\frac{Cov(\Sigma_i, \Sigma_j)}{\Sigma_i \Sigma_j}\right] \tag{16}$$

Then

$$\left(\frac{\Delta R}{R}\right)^2 = \underline{P}\ \underline{C}\ \underline{P}^t \quad , \tag{17}$$

and the quantity of final interest, as computed by multigroup sensitivity and uncertainty analysis computer codes, is the relative standard deviation of the response,

$$\frac{\Delta R}{R} = \left(\underline{P}\ \underline{C}\ \underline{P}^t\right)^{1/2} \quad . \tag{18}$$

The problem is clearly separated into a design-dependent vector $\underline{P}$, and a cross-section covariance matrix $\underline{C}$ which is dependent only on the data.

Of interest for preliminary scoping studies is the integral sensitivity, defined by

$$S_\Sigma = \sum_i P_{\Sigma_i} \quad . \tag{19}$$

The integral sensitivity can be interpreted as the fractional change in a response from simultaneous unit fractional increases in all Σ_i; viz, a logarithmic derivative.

B. Secondary Energy and Angular Distributions

For brevity we will consider only secondary-energy-distribution (SED) sensitivity theory; the development for secondary angular distributions is directly analogous. Gerstl observed[4,5] that if one looks at the adjoint parallel to the computation of cross-section sensitivity, an SED sensitivity immediately results.

Starting with the adjoint expression for R,

$$\begin{aligned} R &= \langle \phi^*, S \rangle \\ &= \langle \phi^*, L\phi \rangle \quad , \end{aligned} \tag{20}$$

one can define a quantity

$$P^{SED}_{\Sigma_i\ E',E} \triangleq \frac{\langle \phi^*, L_i \phi \rangle_{E',E}}{R} \quad , \tag{21}$$

where i represents a specific transfer matrix component in the scattering-in integral of the transport operator (e.g.; i = elastic or i = n,2n) and $\langle , \rangle_{E',E}$ denotes integration over all phase space except E' and E. Writing out Eq. (21) explicitly gives

$$P^{SED}_{\Sigma_i\ E',E} = \frac{1}{R}\int d\vec{r} \int d\vec{\Omega} \int d\vec{\Omega}'\, \phi^*(\vec{r},\vec{\Omega},E)\,\Sigma^i(\vec{r},\vec{\Omega}'\to\vec{\Omega},E'\to E)\,\phi(\vec{r},\vec{\Omega}',E') \quad . \tag{22}$$

Equation (22) can be interpreted physically in complete analogy to P_{Σ_i} in Eq. (8) as the percent change in R due to a unit percent change in Σ^i. In a multigroup representation a two-dimensional array results, where the incident energy E'∈g' is considered as a parameter. In other words, for each incident energy group, g', a sensitivity profile is computed as a function of the secondary

neutron energy E. Integrating Eq. (22) over E'ε g', we can write

$$P^{SED}_{\Sigma^i_{g',g}}(E\varepsilon g) = \frac{\partial R/R}{\partial \Sigma^i_{g'\to g}/\Sigma^i_{g'\to g}} , \tag{23}$$

as the SED sensitivity profile for incident neutrons in group g' as a function of secondary energy group g. These SED sensitivity profiles are always non-negative because they include no loss term. Gerstl[4] gives multigroup discrete-ordinates equations for $P^{SED}_{\Sigma^i_{g',g}}$ and shows representative plots of $P^{SED}_{\Sigma^i_{g'}}/\Delta u_g \Delta u_{g'}$, the doubly-differential SED sensitivity profiles, where g' is a parameter and E is the independent variable.

In order to provide a manageable framework for applying the above formalism in practice, Gerstl defines integral SED sensitivities in analogy to Eq. (19), but with an added concept to characterize the secondary energy distribution. After defining a median-energy group g_m as that group into which the median energy of the secondary energy distribution falls, the distribution itself is divided into a low-energy ("cold") and high-energy ("hot") portion. The integral sensitivity

$$S^{SED}_{g'} = \sum_{g=1}^{g_m} P^{SED}_{g',g} - \sum_{g=g_m+1}^{G} P^{SED}_{g',g} \begin{cases} > 0 \Rightarrow \text{HOT} \\ \\ \leq 0 \Rightarrow \text{COLD} \end{cases} \tag{24}$$

reduces the SED sensitivity to one integral parameter which is "hot" or "cold" depending upon whether $S^{SED}_{g'}$ is positive or negative. That is, $S^{SED}_{g'}$ is a quantitative measure of how much more sensitive the response is to the "hot" secondary neutrons than to the "cold" ones.

Quantification of the uncertainty, ΔR/R, resulting from SED uncertainties, proceeds in parallel to that for cross sections. First, one can define a fraction, f, by which the hot portion of the spectrum is increased and the cold portion correspondingly decreased; i.e.,

$$\frac{\delta\sigma_{g'\to g}}{\sigma_{g'\to g}} = \alpha_m f_{g'} \qquad \alpha_m = \begin{cases} +1 , & g \leq g_m \\ -1 , & g > g_m \end{cases} . \tag{25}$$

Formally, one can then write the variance of the response as[4]

$$\left(\frac{\Delta R}{R}\right)^2_{SED} = \sum_{i,j} S^{SED}_i S^{SED}_j \mathrm{Cov}(f_i, f_j) . \tag{26}$$

Of more immediate practical interest is the change in response associated with an estimated change in an SED,

$$\left(\frac{\delta R}{R}\right)_{SED} = \sum_{g'} S^{SED}_{g'} f_{g'} . \tag{27}$$

III. SELECTED RESULTS FROM SENSITIVITY STUDIES

As is noted in one of the first comprehensive sensitivity and uncertainty analysis for a fusion reactor,[13,18] there are three essential steps to providing a rational basis for cross-section measurement or evaluation priorities; viz, 1) specifying the accuracy required in predicting important nuclear design parameters, 2) determining the sensitivity of these nuclear design parameters to selected cross sections, and 3) making quantitative estimates of the uncertainty of currently available cross-section data (i.e., covariance data). A final step, the performing of an uncertainty analysis, is of course implied. The first step is largely outside the domain of sensitivity analysis, but is an extremely important interface with the design project that must be initiated prior to commencement of the sensitivity analysis. Once the accuracy criteria are set, the sensitivity analysis can begin if a preliminary design model exists. Due to the large number of cross-section data needed for fusion reactor nucleonics calculations, it is clear that complete covariance data cannot be provided in a short time frame. Perhaps even more difficult a task is improving, within a short time frame, data which are found to be deficient. Thus, the initial sensitivities determined for a preliminary design can be used to semiquantitatively limit the scope of subsequent uncertainty analysis. That is, at this time in the evolution of uncertainty analysis the preliminary sensitivity studies guide the assignment of priorities for covariance data evaluations. In the future, when extensive covariance files are available in ENDF, the sensitivity and uncertainty analyses may be performed contiguously in time, but such is far from the case today.

The following review illustrates the methodology used for sensitivity studies in several cases - the TFTR, EPR, and NUWMAK designs. A detailed discussion is given for the TFTR, an experimental device now under construction. Then the sensitivity of two EPR designs are discussed and summarized. Although the EPR design studies were superseded by reactor concepts called TNS, which were subsequently superseded by present design studies of a fusion Engineering Test Facility (ETF), the resulting cross-section requirements are still mostly relevant.

A. TFTR

The first step in performing a sensitivity analysis is selection of a nuclear design model, which includes the material zones in which responses of interest are to be computed. A one-dimensional computational model used for TFTR nucleonics calculations is shown in Fig. 1. Since the main objective of the TFTR is to demonstrate the scientific feasibility of a tokamak fusion reactor, it is not required to breed tritium, and therefore does not employ a lithium blanket. The reactor is expected to operate in a pulsed mode, yielding a maximum of 1 000 pulses per year and generating a maximum neutron fluence of 1.4×10^{19} fusion neutrons per m^2 per year on the first wall.[20] Due to this low neutron fluence, radiation damage or nuclear heating problems are not of major concern. However, the activation of magnet coils, structural materials, and instruments is considered a major nucleonics problem area; in particular, the generation of long-lived radioactive isotopes. Therefore, and for biological shielding reasons, a radiation shield is provided as close to the plasma as possible. In cooperation with Princeton and Westinghouse, ten threshold activation reactions in the structural material (zones 9 and 11 in Fig. 1) and the main copper coil (zone 10 in Fig. 1) were selected as important nuclear design parameters of interest. Our objective was to estimate the uncertainties introduced in the calculation of these activation rates due to estimated errors in the neutron cross sections of the system. Of particular interest are uncertainties in the cross sections of the shield zone 7, which consists of a lead-borated polyethylene, and uncertainties in the activation cross sections themselves.

In order to calculate the sensitivity profiles P_{Σ_i} and $P_{\Sigma_i^R}$ according to Eq. (6), where Σ_i^R is the ρ_i of Eq. (6), we performed a forward transport calculation for the TFTR model of Fig. 1 and an adjoint calculation for each of the ten activation reactions considered, thus determining the angular fluxes ϕ and ϕ^*. All transport calculations were performed with the one-dimensional S_n code DTF-IV in an S_8 approximation, using 20-group P_3 neutron cross sections. This cross-section set covers neutron energies between 2.02 and 14.92 MeV, which is sufficient for the activation reactions considered. Cross sections and covariance data for the activation reactions were evaluated at LASL.[21] The angular fluxes ϕ and ϕ^* from the transport calculations were then used in the LASL sensitivity code SENSIT-1D to evaluate Eqs. (6) and (19), and to plot the sensitivity profiles of interest.

Integral sensitivities of all ten activation reactions to all significant transport cross sections in the TFTR were calculated and found to be all negative, indicating that an increase in such cross sections would cause the respective activation rate to decrease. The largest integral sensitivity found is that of ^{65}Cu (n,p)^{65}Ni to the copper cross sections, which indicates that a 1% increase in the total cross section of copper would decrease the ^{65}Ni production in the coil by 2.05%.

Since explicit covariance matrices could be produced for only a limited number of partial cross sections (called "transport" cross sections in this analysis to distinguish them from the activation cross-section used as a response function) and for all activation cross sections, it was necessary to use upper limit estimates for many "transport" cross-section errors, $(\Delta\Sigma/\Sigma)_{max}$. Upper limit uncertainties are then computed by

$$\left(\frac{\Delta R}{R}\right)_{max} = \hat{S}_\Sigma \left(\frac{\Delta\Sigma}{\Sigma}\right)_{max} , \tag{28}$$

where

$$\hat{S}_\Sigma = \sum_i |P_{\Sigma_i}| . \tag{29}$$

Table I gives the results of applying Eqs. (14), (28), and (29) for two reactions of interest, denoted

$$R_1: \ ^{54}\mathrm{Fe(n,p)}^{54}\mathrm{Mn}$$

and

$$R_{10}: \ ^{65}\mathrm{Cu(n,p)}^{65}\mathrm{Ni} .$$

In order to obtain the predicted response uncertainties in each of the ten activation rates due to the cross-section error estimates, it was assumed that the cross-section errors are uncorrelated among the partial cross-sections and materials listed in Table I; i.e.,

$$\frac{\Delta R_i}{R_i} = \left[\sum_k \left(\frac{\Delta R_i}{R}\right)_k^2\right]^{1/2} , \tag{30}$$

where k denotes a particular partial cross section and material. Table II shows the results of this quadratic combination of errors, as well as those due to the response function (activation cross section) errors, $\Delta\Sigma_i^R$. The last two colums in Table II are the result of a further quadratic combination of the "transport" and activation cross-section errors. Note that the final uncertainty in reaction rates is due overwhelmingly to estimated "transport" cross-section errors, primarily because of the conservatism inherent in the calculation of $(\Delta R/R)_{max}$ via Eq. (28). In Table II the zone numbers are abbreviated as, for example, Z9 for zone 9. Also Al was treated as an alternative to steel in Z9 and Z11.

Having estimates of the reaction rate uncertainties, the question then is whether these are within acceptable bounds. However, a nuclear designer is not concerned with activation rates, but rather with biological dose-equivalent rates. Thus, in conjunction with the designers, a criterion was established that the maximum allowable uncertainty (standard deviation) in personnel radiation exposure rates should be 50%. The absolute reaction rates were then used to compute exposure rates, E, shielded and unshielded, along with their corresponding uncertainties. Shielding was specified to satisfy the designers' criteria:

$$E < \begin{cases} 100 \text{ mrem/h at 2 h after 1 pulse} \\ \\ 10 \text{ mrem/h at 1 d after 1 y operation} . \end{cases} \tag{31}$$

Table III shows the results of the analysis, where the ΔE_i are calculated analogously to ΔR_i in Eq. (30). However, in summing uncertainties ΔE_i over all indivicual isotopes i, care must be taken to observe possible correlations. First, all "transport" cross-section errors were assumed to be uncorrelated with all activation cross-section errors, so the ΔE_i can be computed by quadratic combination of these errors. But the "transport" cross-section errors generate an error in the flux ϕ used to calculate the reaction rates R_i. Clearly then the uncertainties in the R_i's due to "transport" cross-section errors are fully correlated and should be summed linearly over i. Further, it appears reasonable to assume that the activation cross-section (response function) errors are totally uncorrelated, because they are in general independently measured and evaluated. The total uncertainty, ΔE, from these considerations can be written

$$\Delta E = \left\{ \left[\sum_i E_i \left(\frac{\Delta R_i^{trans}}{R_i} \right) \right]^2 + \sum_i E_i^2 \left(\frac{\Delta R_i^{act}}{R_i} \right)^2 \right\}^{1/2} . \tag{32}$$

In conclusion, the uncertainty in the TFTR dose rates is 41.4% for the most stringent exposure rate criteria (10 mrem/h at 1 d after 1 y operation) and 49.3% for the less stringent criteria, as can be seen in the bottom line of Table III. These values just barely meet the allowable criterion of 50%, but have a known conservatism in many of the $(\Delta\Sigma/\Sigma)_{max}$ estimates. However, if the allowable uncertainty criterion had been more stringent, the uncertainty analysis could have been traced backward from the largest contributors to ΔE in Table III (e.g., ^{59}Co and ^{54}Mn) to their production reactions. An examination of the sensitivity profiles for the production reactions and the corresponding covariance data would then give insight into which reaction cross sections and energy ranges are potential candidates for additional measurement or evaluation.

B. EPR, TNS, etc.

After no unacceptable cross-section uncertainties were found in the TFTR study, attention was turned to a possible first generation of power producing reactors, the EPR designs. The EPR designs extant, as well as later conceptual studies of a TNS or Ignition Test Reactor (ITR), are generically similar in many respects. For example, they have superconducting toroidal field (TF) coils in which several key response functions are of interest. Also, iron (or stainless steel), borated hydrogenous materials, or B_4C are used for shielding the TF coils.[6,16,17]

For the LASL assessment task,[16,17] we chose the EPR design described in Ref. 22 and in private communications. The design has two shield assemblies, denoted "inner" and "outer". The inner shield refers to a segment of shielding toward the toroidal axis. Figure 2 shows a one-dimensional model based upon a radial traverse from the poloidal axis (plasma centerline) through the inner shield. The thinner inner shield is of effective but costly stainless steel/B_4C, while the thicker outer shield is composed largely of less costly lead mortar. The technical basis for alternative shields is in magnetic field profile considerations. With the D-shaped toroidal field (TF) coils, there exists a relatively large space for the outer shield, whereas the inner shield must be as thin as possible.

At this point we consider the general approach used in the EPR data assessment. First, a broad-ranging sensitivity study was performed simply using the total, scattering (matrix) and absorption cross sections from the transport code cross-section sets. These included neutron interaction, gamma-ray production, and gamma-ray scattering matrices. From the large mass of these survey calculations, which are automated in the LASL system,[17] we then isolated materials, partial cross sections and energy regions of potential interest. This latter step is greatly assisted by computing integral sensitivities. After a semiquantitative review of the germane cross-section errors, we chose a manageable number of potentially important materials and partial cross sections for more detailed error evaluation. For these we processed available covariance data into multigroup form.

Cross-section covariance data were obtained by processing preliminary ENDF/B-V data into thirty energy groups (cf. Ref. 23 for group structure) with the NJOY multigroup processing code. The ENDF/B-V data are still preliminary at this date, so the multigroup covariance matrices are subject to change. Many errors (mistakes) were discovered and corrected in the processing of the ENDF/B-V covariance data. Several deficiencies still exist in ENDF/B-V ; e.g., no covariance data exist for Cu, and such data for ^{10}B extend only up to 1.02 MeV. The latter deficiency is not significant for the EPR analysis,[6] however, because the important (sensitive) energy range for ^{10}B lies mostly from approximately 10 keV to 1 MeV. In order to perform a preliminary uncertainty analysis for the EPR and TNS, the covariance data for Cr were adapted as an approximation for the Cu data. Table IV lists those 30-group covariance matrices currently available.[24]

Because of the thinner inner shield, radiation effects in the inner TF coils are more critical[22] than in the outer TF coils. However, for access during maintenance the outer structure and TF coil activation are important, as opposed to the inner. Thus, for our analysis we chose four radiation effects in the inner TFC, and activation of the stainless steel outer dewar. Specifically, we considered:

INNER SHIELD: 1) neutron and gamma-ray heating in the TF coil superconductor, 2) neutron and gamma-ray lose to the MYLAR insulation in the TF coils, 3) displacements per atom (dpa) in the Cu matrix of the TF coils, and 4) transmutation of the Cu matrix.

OUTER SHIELD: 1) activation of the stainless steel (SS) dewar [e.g., $^{58}Ni(n,p)^{58}Co$ or $^{56}Fe(n,p)^{56}Mn$].

Details of all the response functions, as well as sensitivites, etc., are presented in Ref. 6. In this paper only selected sample results are presented.

As a sample case, let us consider the total neutron and gamma-ray heating in the inner TF coil. Table V shows the integral sensitivities, Eq. (19), for this response, to SS total cross sections. From this table we find the region(s) in Fig. 2 which contribute most to the sensitivity. It is worth noting that these data also give insight into the sensitivity of the response to design alterations in these regions. From Table V it is clear that the blanket SS regions 6-8 are most important. Also, it can be seen that Fe is the largest contributor to the integral sensitivities, regardless of which region is considered.

Narrowing our example further we show in Table VI the component sensitivities for Fe in regions 6-8. Here the sensitivity has been divided into the gain term and loss term (cf. Ref. 18, App. B for details)

$$P_{\Sigma_i} = -P_{\Sigma^{tot}_{i,loss}} + P_{\Sigma^{scat}_{i,gain}} .$$

In this case most of the net integral sensitivity is clearly due to the neutron scattering cross section. Thus, the uncertainty analysis should concentrate especially on Fe, and in particular on the scattering cross sections.

A representative sensitivity profile is shown in Fig. 3, where again the sensitivity of the TF coil heating to the Fe scattering cross section was selected. Notice the high sensitivity in the top two groups, with a subsidary peak below 1 MeV. This general shape is characteristic of all the sensitivity profiles, for all responses and all materials pertaining to this EPR design.

Referring again to Table VI, the low sensitivity to the gamma-ray production cross section, $\Sigma_{(n\rightarrow\gamma)}$, is caused by the relatively short mean free path of the gamma-rays in SS. However, the sensitivity increases monotonically as the region approaches the TF coil.

Turning now to the B_4C component of the shield, Table VII presents integral sensitivity results comparable to those of Table V for SS. Here we see that the sensitivity is highest for the outboard regions, where the neutron spectrum is softened somewhat. However, the spatial variation is not nearly as strong as for Fe (cf. Table V). Also, the ^{10}B component of the B_4C does not overwhelmingly dominate the sensitivity as does Fe in SS. As would be expected, the net integral sensitivity is in all cases negative, because almost any interaction decreases the probability of a neutron's transmission to the TF coil.

Sensitivity profiles for the B and C cross sections show the same general shape as those for Fe (Fig. 3), with a peak in the top group and another peak in the 100 keV-1 MeV region. For ^{10}B, however, the sensitivity to the total cross section is of comparable magnitude in the two peaks, and the lower peak is much broader. This high sensitivity at the lower energy peak is due in part to the neutron spectrum, which shows this same peak at all positions in the shield regions.[10-18] One can conclude that even though these lower energy neutrons have lower transmission probabilities to the TF coil, they are so prevalent in the spectrum as to be a major contributor to the neutron and gamma-ray flux reaching the TF coil.

As a final example from our detailed sensitivity analysis[6] of the EPR, consider the sensitivity of heating in the TF coils to the cross sections in the TF coil region itself. The response here is in the inboard edge (first mesh interval) of the TF coil, while the sensitivity is to cross sections in the entire region 24. The analysis shows a very low sensitivity to all neutron cross sections except for

Cu. This is to be expected because interactions in the TF coil itself do not significantly alter the probability of a neutron contributing to heating at the inboard edge of the coil. Although it is of somewhat academic interest (because of the precision with which gamma-ray interaction cross sections are known), a relatively high negative sensitivity to Cu gamma-ray interaction cross section is as expected.

Several major conclusions were reached in the sensitivity and uncertainty analysis for an EPR. First, the wide ranging survey calculations, using transport-code cross sections, have provided a rapid and thorough coverage of all materials and regions of potential interest. This has proven to be an effective way of eliminating the need for further analyses of many partial cross-section sensitivities. From a pragmatic viewpoint, these partials are of interest only if they provide significant contributions to the total sensitivity, and have significant errors associated with them.

The complete sensitivity analysis[6] indicates that the scattering cross sections of Fe and Cu, along with the absorption cross sections of the ^{10}B in B_4C, are the most significant contributors to the integral sensitivities of the responses considered. Of somewhat lesser importance were the scattering cross sections of H, C, and Pb.

A similar study[16] for an alternative EPR design concentrated on sensitivities to C and Fe partial cross sections. The integral sensitivities of TF coil heating to Fe and SS total cross sections, as an example, are quite similar for the two different designs; viz, -7.55 from Ref. 16 vs -7.375 in Table V. Using preliminary ENDF/B data for C covariances, the authors of Ref. 16 found $\Delta R/R$ to be approximately 2% for all three responses they considered. On the other hand, they assumed $\Delta\sigma_i$ values for several partial cross sections of Fe that, along with assumed correlation information, gave $\Delta R/R$ values of 99 to 110% (testing the limits of applicability of linear perturbation theory). Although some of the assumed covariances for Fe leave a wide latitude for revision as newer data are incorporated, the uncertainties in responses will probably remain appreciable. No definitive design criteria have been set for the various responses, but uncertainties of approximately 100% are in most cases almost certainly unacceptable. Values for acceptable nuclear heating and dpa uncertainties in the TF coils are more likely to be in the 10-20% range,[23] so clearly Fe is a prime candidate for further uncertainty analysis.

C. NUWMAK

Recently a sensitivity and uncertainty analysis has been reported[16] for a conceptual commercial power reactor design, the NUWMAK. A schematic drawing of the reactor poloidal cross section is shown in Fig. 4, which is reproduced from Ref. (19). The reactor is a moderately sized tokamak power reactor(~1 GWe) which has evolved from a series of comprehensive conceptual design studies at the University of Wisconsin. An eutectic $Li_{62}Pb_{38}$ compound is used in the blanket for breeding and thermal inertia purposes. Also, different inner and outer shields are used, for the same reasons as mentioned above for an EPR design.

Referring again to Fig. 4, several features of the design are germane to the sensitivity analysis. Unlike the TFTR/EPR/TNS designs, the NUWMAK employs low-activation materials (H, B, C, Li, Ti, Pb) for all regions except the inner W shield. Also, 90% of the tritium breeding was found[19] to be contributed by $^6Li(n,t)^4He$ reactions. Another very pertinent result of the design study was that the most restrictive criterion for the inner shield was the resistivity change of the TF coil Al stabilizer, caused by the Al displacement rate of 2×10^{-5} dpa/y. The inner shield is only 1.0-m thick and must attenuate the neutron intensity by a factor greater than 10^8.

The sensitivity study in Ref. (19) goes beyond the determination of response uncertainties, to address the cost/benefit analysis of integral measurements proposed to reduce the uncertainties. The theory and results presented in the latter area, although they provide a continuity to uncertainty methods, are beyond the scope of this review.

Sensitivity analysis of NEWMAK used the same methodology as discussed in Secs. III.A and III.B, employing the ANISN one-dimensional discrete-ordinates code for S_4P_3 neutron transport calculations, and SWANLAKE for the sensitivity calculations. Wu and Maynard chose six key responses for analysis, as shown in Table VIII. They caution the reader to interpret the results carefully, because the table only includes the second, or indirect term in Eq. (6) of Sec. II.A. For example, the large negative sensitivity of R_1 to the ^6Li total cross section (-0.86) is counterbalanced by a +0.9 sensitivity from the direct effect on the $^6Li(n,t)^4He$ response function, for a net sensitivity of only +0.035.

The responses of most practical interest are R_5 and R_6 in Table VIII, which have the higher integral sensitivities and, in the case of R_6, is design limiting. It was observed that the (n,2n) cross sections of W and Pb are the dominant contributors to the sensitivity, with all of the sensitivity concentrated in the higher energy groups and peaking in the top group. In performing the uncertainty analysis, however, data covariances for only four applicable materials -- ^7Li, ^{11}B, Ti and W -- were available in ENDF/B-V (cf. Table IV). Therefore, the authors assumed all uncorrelated uncertainties at all energies for ^7Li, ^{11}B, Ti and W. Their uncertainty results are presented in Table IX, where the uncertainties in R_5 and R_6 are overwhelmingly caused by W cross-section uncertainties. Clearly, for this reactor a major improvement in the shield design would result from improved accuracy in the W cross sections. Curiously enough, in discussing cross-section evaluation and measurement priorities, it was surmised[27] that W would also become a "priority 1" material if used for the inner shield of a TNS.

D. CROSS-SECTION REQUIREMENTS ABOVE 14 MeV

In a departure from sensitivity and uncertainty analysis per se, we consider here several aspects of cross-section data above ~ 14 MeV. With two exceptions,[1-3,29] the author is not aware of any sensitivity studies in this energy region. Reference 25 alludes to a sensitivity study of dose-equivalent through thick shields, to elastic and nonelastic cross sections, but no literature regarding the study is cited. The second study[29] was performed for D-Be source neutrons in a medical application, where sensitivity methods in LASS[1,2] were used to optimize the thickness of a collimator.

The overwhelming interest in cross sections above ~ 14 MeV presently seems to be associated with the Fusion Materials Irradiation Test (FMIT) Facility design project. This facility will have a deuteron beam of ~ 35 MeV incident on Li, with a resulting spectrum at 0° which peaks at ~ 14 MeV and has a high-energy tail to ~ 50 MeV. Although the spectrum is roughly bell-shaped, experiments have verified a knee in the curve at ~ 35 MeV, producing more neutrons than originally expected in the energy region where the neutrons are most penetrating. In a discussion of the bulk shielding for the FMIT facility, Carter and Morford[28] emphasize that the most severe problem in the shield design is uncertainties in the cross-section data base ≥ 14 MeV.

As mentioned in a previous paper,[27] there has not been much technological activity requiring neutronics data at ≥ 14 MeV. A lack of demand coupled with the lack of widely available monoenergetic neutron sources has restricted the amount of such data available. The FMIT facility has brought forth the importance of remedying this situation, with concomitant demands for careful selection of priorities. It is unlikely that the cross-section needs for shielding, activation, spectrum tailoring, radiation damage, and dosimetry can all be met by the projected

operation date of the FMIT. Satisfying even the minimum needs will require a well planned program with strict priorities, concentrating on nuclear model calculations to fulfill most requirements.

Any listing of relative importance of particular nuclides and reaction types must be associated with neutronics applications of those data. For example, in studies of radiation-induced damage, the fact that important damage cross sections are only weakly energy dependent above ~ 14 MeV makes it likely that most damage will be caused by neutrons in the 14-25 MeV region, where most of the > 14 MeV source neutrons originate. Similarly, the dosimetry reactions will need to be determined with highest accuracy in this 14-25 MeV region.

In contrast to damage and dosimetry reactions, cross-section data in the 30-50 MeV region are the most important for bulk shielding calcualtions. It was determined[28] for the FMIT facility, where concrete shields 3 to 4 metres thick were analyzed, that ~ 90% and ~ 70% of the dose-equivalent are due to source neutrons with energies greater than 30 MeV and 40 MeV, respectively. A removal cross section was then defined as the sum of the nonelastic cross section and that portion of the elastic cross section scattering neutrons beyond 25°. It is because this removal cross section is a monotonically decreasing function of energy that the dose-equivalent is dominated by the higher energy neutrons. The authors state[28] that O and Fe are the most important elements in their shield design, and measurements at a few incident energies between 20 and 50 MeV are now being made for these elements.

IV. CONCLUSIONS

The usefulness of sensitivity studies to help define cross-section evaluation and measurements requirements is indisputable. However, much remains to be done before such studies can be made comprehensive and complete. While the theoretical methods and codes are generally adequate for simple one-dimensional reactor models considered heretofore, an extension to multidimensional and complex models is imminently required. In particular, Monte Carlo sensitivity methods promise great advantages in complex geometries, especially the important streaming problems already uncovered in fusion reactor nucleonics. Even more important than methods and codes is the urgent need for extensive covariance data files. Additional large data evaluation requirements are being elicited by the recently developed SED sensitivity methods, which require some characterization of secondary energy distribution uncertainties, perhaps in the form of the f_g, factors discussed in Sec. II.B.

Results of sensitivity studies to date were summarized in Sec. III, but it is useful to re-emphasize the recurring importance of the Fe cross sections in both fusion reactor and irradiation facility shields. In the case of some inner shields for tokamak reactors, the overwhelming dominance of uncertainties in the W cross sections is clearly seen for responses in the TF coils. The large uncertainties (40-100%) in TF coil responses found for several conceptual reactor designs are understandable in terms of the large attenuations of neutron and gamma-ray fluxes involved - generally > 10^6. Although not reviewed in this paper, a hybrid reactor sensitivity study[1b] showed appreciable integral sensitivities of tritium breeding to ^{238}U and Fe total cross sections; viz, -0.97 and -0.19, respectively. In this case Fe was included only in SS as a 5-mm first wall and as an 8.6 v/o structure in fission and breeding zones. Another study[9] of tritium breeding sensitivity, in this case for a pure fusion reactor, showed fairly low values of sensitivity to ^6Li, ^7Li, and Nb cross sections. This study also presented a comparison of the response uncertainty as computed by both the methods of Sec. II and direct recalculation. As must be expected for total uncertainties in tritium breeding of < 5%, the agreement is very good. A further result of this study, interesting in light of the current questions concerning the $^7Li(n,n't)^4He$ cross section,[30] was that most of the sensitivity is attributable to just that cross section.

A growing interest in D-Li neutron sources for fusion materials irradiation experiments has intensified interest in neutron cross-section data above 14 MeV. Since the status review of these data at a Symposium in May 1977 (cf. Ref. 27), model calculations[28,29] have been used to devise cross sections for shielding analysis of the FMIT facility. For shielding applications the data in the 30-50 MeV range are most significant analogous to fission reactors where source neutrons of ~ 6-8 MeV dominate for deep penetrations. By contrast, for dosimetry, damage functions, and neutron transport in the target area of the FMIT facility, data in the 14-25 MeV region are expected[27] to be most important.

V. ACKNOWLEDGMENT

The auther is pleased to acknowledge many helpful comments by S. A. W. Gerstl and P. G. Young of LASL. Also, the comments of C. W. Maynard of the University of Wisconsin, along with his permission to reproduce figures and tables from a preprint of Wu and Maynard's forthcoming paper, are gratefully acknowledged.

REFERENCES

1a. V. V. Kotov, C. W. Maynard, D. V. Markovskii, and G. E. Shatalov, "Analysis of the Sensitivity of Hybrid Reactor Parameters to Nuclear Data," I. V. KURCHATOV INSTITUTE OF ATOMIC ENERGY report IAE-2817 (English translation LA-TR-78-6[illegible] by A. D. Cernicek, Los Alamos Scientific Laboratory.)

1b. Long-Poe Ku and W. G. Price, Jr., "Neutronic Calculations and Cross-Section Sensitivity Analysis of the Livermore Mirror Fusion/Fission Hybrid Reactor Blanket," Princeton Plasma Physics Laboratory report PPPL-1370 (1977).

2. D. W. Muir, "Sensitivity of Neutron Multigroup Cross Sections to Thermal Broadening of the Fusion Peak," Proc. First Topical Meeting on Technology of Controlled Nucl. Fusion, San Diego, CA, 16-18 Apr. 1974, CONF-740402.

3. R. T. Santoro and J. Barish, "Cross-Section Sensitivity of the D-T Fusion Probability and the D-T and T-T Reaction Rates," Oak Ridge National Laboratory report ORNL-TM-4933 (1975).

4. S. A. W. Gerstl, "Sensitivity Profiles for Secondary Energy and Angular Distributions," Proc. Fifth Intl. Conf. on Reactor Shielding, Knoxville, TN, 18-22 Apr. 1976.

5. S. A. W. Gerstl, "Uncertainty Analysis for Secondary Energy Distributions," Proc. RSIC Seminar on Theory and Application of Sensitivity and Uncertainty Analysis, Oak Ridge, TN, 23-24 Aug. 1976.

6. E. L. Simmons, S. A. W. Gerstl, and Donald J. Dudziak, "Cross-Section Sensitivity Analyses for a Tokamak Experimental Power Reactor," Los Alamos Scientific Laboratory report LA-6942-MS (1977).

7. David Leon Prezbindowski, "An Analysis of the Effects of Cross Section Uncertainties on the Multitable S_n Solution of Neutron Transport through Air." Doctoral Dissertation Purdue University (January 1968). Cf. also Trans. Am. Nucl. Soc. 11, 193 (1968).

8 R. Conn and W. M. Stacey, Jr., "Variational Methods for Controlled Thermonuclear Reactor Blanket Studies," Nucl. Fus. 13, 185 (1973).

9. D. E. Bartine, R. G. Alsmiller, Jr., E. M. Oblow, and F. R. Mynatt, "Cross-Section Sensitivity of Breeding Ratio in a Fusion-Reactor Blanket," Nucl. Sci. Eng., 53, 304 (1974).

10. D. E. Bartine, E. M. Oblow, and F. R. Mynatt, "Radiation-Transport Cross-Section Sensitivity Analysis -- A General Approach Illustrated for a Thermonuclear Source in Air," Nucl Sci. Eng. 55, 147 (1974).

11. S. A. W. Gerstl, "Second-Order Perturbation Theory and its Application to Sensitivity Studies in Shield Design Calculations," Trans. Am. Nucl. Soc. 16, 342 (1973).

12. S. A. W. Gerstl, "Blanket Design and Cross-Section Sensitivity Calculations Based on Perturbation Methods," Proc. First Topical Meeting on Technology of Controlled Nucl. Fusion, San Diego, CA, 16-18 Apr. 1974. (CONF-740402-P2, p. 136).

13. S. A. W. Gerstl, D. J. Dudziak, and D. W. Muir, "Application of Sensitivity Analysis to a Quantitative Assessment of Neutron Cross-Section Requirements for the TFTR: An Interim Report," Los Alamos Scientific Laboratory report LA-6118-MS (1975).

14. R. G. Alsmiller, Jr., R. T. Santoro, J. Barish, and T. A. Gabriel, "Comparison of the Cross-Section Sensitivity of the Tritium Breeding Ratio in Various Fusion Reactor Blankets," Nucl. Sci. Eng. 57, (1975).

15. S. A. W. Gerstl, D. J. Dudziak, and D. W. Muir, "The Application of Sensitivity Analysis to Nuclear Data Assessment," Proc. Specialist's Mtg. on Sensitivity Studies and Shielding Benchmarks, Paris, France, 7-10 Oct. 1975.

16. R. G. Alsmiller, Jr., J. Barish, and C. R. Weisbin, "Uncertainties in Calculated Heating and Radiation Damage in the Toroidal Field Coil of a Tokamak Experimental Power Reactor due to Neutron Cross-Section Errors," Oak Ridge National Laboratory report ORNL/TM-5198 (1976).

17. Donald J. Dudziak, S. A. W. Gerstl, and D. W. Muir, "Application of the Sensitivity and Uncertainty Analysis System LASS to Fusion Reactor Nucleonics," Proc. Specialists' Meeting on Differential and Integral Nuclear Data Requirements for Shielding Calculations, Vienna, Austria, 12-16 Oct. 1976, IAEA-207.

18. S. A. W. Gerstl, Donald J. Dudziak, and D. W. Muir, "Cross-Section Sensitivity and Uncertainty Analysis with Application to a Fusion Reactor," Nucl. Sci. Eng. 62 (1), 137 (1977).

19. T. Wu and C. W. Maynard, "The Application of Uncertainty Analysis in Conceptual Fusion Reactor Design," Proc. RSIC Seminar on Theory and Application of Sensitivity and Uncertainty Analysis, Oak Ridge, TN, 23-24 Aug. 1978.

20. "TCT-Two-Component Torus," joint conceptual design study performed by Princeton Plasma Physics Laboratory and Westinghouse Electric Corp., Vol. III, Sec. 6.1 (1974).

21. D. W. Muir in "Applied Nuclear Data Research and Development Quarterly Progress Report, July 1-Sept. 30, 1974," Los Alamos Scientific Laboratory report LA-5804-PR (1974).

22. M. A. Abdou, "Nuclear Design of the Blanket/Shield System for a Tokamak Experimental Power Reactor," Nucl. Technol. 29, 7 (1976).

23. H. A. Sandmeier, G. E. Hansen, R. E. Seamon, T. J. Hirons, and A. H. Marshall, "Coupled Neutron-Gamma Multigroup-Multitable Cross Sections for 29 Materials Pertinent to Nuclear Weapons Effect Calculations Generated by LASL/TD Division," Los Alamos Scientific Laboratory report LA-513[illegible] (1974).

24. R. J. LaBauve and D. W. Muir, Los Alamos Scientific Laboratory, private communciation (1978).

25. D. J. Dudziak (chairman), "Report of the Sub-group on Fusion Reactors," Proc. Specialists' Meeting on Differential and Integral Nuclear Data Requirements for Shielding Calculations, Vienna, Austria, 12-16 Oct. 1976, IAEA-207.

26. E. T. Cheng and C. W. Maynard, "Nucleonic Design for a Compact Tokamak Fusion Reactor Blanket and Shield," Trans. Am. Nucl. Soc. 30, 73 (1978).

27. Donald J. Dudziak and D. W. Muir, "Review of Magnetic Fusion Energy Neutron Cross-Section Needs: Neutronics Viewpoint," Proc. Symposium on Neutron Cross Sections from 10-40 MeV, Upton, NY, 3-5 May 1977.

28. L. L. Carter and R. J. Morford, "Shielding Calculations for the Fusion Materials Irradiation Test Facility," Trans. Am. Nucl. Soc. 30, 618 (1978).

29. William Bradley Wilson, "Nuclear Data Development and Shield Design for Neutrons Below 60 MeV," Los Alamos Scientific Laboratory report LA-7159-T (1978).

30. Donald J. Dudziak and Gene L. Woodruff, "Nucleonic Aspects of Synfuel Blankets," Los Alamos Scientific Laboratory report LA-7485-MS (1978). (Cf. Addendum on ^{7}Li Cross-Section Uncertainty).

TABLE I

Predicted Uncertainties of Selected Activation Rates R_1 and R_{10} Due to Estimated Errors in Transport Cross Sections Σ

"Perturbed" Transport Cross Sections	Error Estimates: COV[a] or $\left(\frac{\Delta\Sigma}{\Sigma}\right)_{max}$ (%)	Maximum Integral Sensitivity $\hat{S}$ and Predicted Activation Rate Uncertainty $\Delta R/R$ for R_1		for R_{10}	
		$\hat{S}$ (% per %)	$\frac{\Delta R}{R}$ or $\left(\frac{\Delta R}{R}\right)_{max}$ (%)	$\hat{S}$ (% per %)	$\frac{\Delta R}{R}$ or $\left(\frac{\Delta R}{R}\right)_{max}$ (%)
C	25	0.87	21.8	0.66	16.5
C(n,n'3α)	COV	---	2.4	---	2.2
Pb	25	1.52	38.0	1.12	28.0
Pb(n, 2n)	COV	---	18.3	---	14.8
O	25	0.47	11.8	0.36	9.0
H	2	1.08	2.2	0.73	1.5
Fe	25	0.70	17.5	0.93	23.2
Fe(n, tot)	COV	---	2.2	---	3.2
Fe(n, abs)	COV	---	0.71	---	1.7
Fe(n,n'cont)	COV	---	4.4	---	7.4
Fe(n, elas)	COV	---	2.5	---	3.7
Fe(n, inel)	COV	---	3.5	---	6.7
Fe(n, 2n)	COV	---	1.2	---	3.6
Cr	25	0.20	5.0	0.25	6.3
Ni	25	0.12	3.0	0.17	4.3
Mn	25	0.021	0.53	0.027	0.68
Al	25	0.45	11.3	0.62	15.5
Cu	25	0.039	0.98	2.05	51.3
Cu(n, elas)	COV	---	0.12	---	5.0
Cu(n, inel)	COV	---	0.13	---	6.8
Cu(n, 2n)	COV	---	0.04	---	9.6
Cu(n, tot)	COV	---	0.12	---	5.1
Cu(n, abs)	COV	---	0.04	---	16.8

[a]COV means Complete Covariance Matrix.

TABLE II

Summary of Predicted Uncertainties of Activation Rates R_i Due to Estimated Errors in Activation Cross Sections, COV(Σ_i^R, Σ_i^R), and All Transport Cross-Section Uncertainties

Activation Reaction R_i	$\frac{\Delta R_i}{R_i}$ (%)				
	Due to Activation Cross-Section Errors	Due to Transport Cross-Section Errors		Due to All Cross-Section Errors	
		Stainless-Steel Structure	Aluminum Structure	Stainless-Steel Structure	Aluminum Structure
R_1 = $^{54}Fe(n, p)^{54}Mn$ in Z9 and Z11	15.7	49.1	---	51.5	---
R_2 = $^{55}Mn(n, 2n)^{54}Mn$ in Z9 and Z11	15.6	41.4	---	44.2	---
R_3 = $^{56}Fe(n, p)^{56}Mn$ in Z9 and Z11	12.8	42.8	---	44.7	---
R_4 = $^{58}Ni(n, p)^{58}Co$ in Z9 and Z11	20.7	42.6	---	47.4	---
R_5 = $^{27}Al(n, \alpha)^{24}Na$ in Z9 and Z11	8.7	---	41.0	---	41.8
R_6 = $^{27}Al(n, p)^{27}Mg$ in Z9 and Z11	5.5	---	44.0	---	44.3
R_7 = $^{63}Cu(n, 2n)^{62}Cu$ in Z10	24.3	62.3	59.9	66.9	64.6
R_8 = $^{63}Cu(n, \alpha)^{60}Co$ in Z10	29.3	63.5	62.8	69.9	69.3
R_9 = $^{65}Cu(n, 2n)^{64}Cu$ in Z10	13.4	63.1	60.7	64.5	62.2
R_{10} = $^{65}Cu(n, p)^{65}Ni$ in Z10	32.6	66.1	63.3	73.7	71.2

TABLE III

Predicted Absolute Uncertainties in Calculated Radiation Exposure Rate Due to All Cross-Section Uncertainties—TFTR Design with Steel Structure

Radionuclide, i	$T_{1/2}$	Production Mechanism	Production Rate, R_i (Atoms per Fusion Neutron)	Exposure Rate $I \pm \Delta I$: All			
				1 Pulse and 2 h		[illegible]	
				E_i (mrem/h)	ΔI_i (mrem/h)	I (mrem/h)	ΔI (%)
^{54}Mn	313 days	$^{54}Fe(n, p)$	1.35 E-3	7.05 E-4	3.63 E-4	4.38 E-1	[illegible] E-1
^{54}Mn	313 days	$^{55}Mn(n, 2n)$	4.80 E-4	2.49 E-4	1.10 E-4	1.72 E-1	[illegible] E-1
^{56}Mn	2.6 h	$^{56}Fe(n, p)$	3.32 E-3	5.11 E+0	2.26 E+0	[illegible] E+0	[illegible] E+0
^{58}Co	71 days	$^{58}Ni(n, p)$	2.30 E-3	6.16 E-3	2.92 E-3	1.67 E-1	[illegible] E-1
^{62}Cu	9.8 min	$^{63}Cu(n, 2n)$	9.89 E-3	6.94 E-1	4.64 E-2	E-2	E-2
^{60}Co	5.2 yr	$^{63}Cu(n, \alpha)$	1.03 E-3	2.30 E-4	1.61 E-4	2.19 E-1	[illegible] E-1
^{64}Cu	12.7 h	$^{65}Cu(n, 2n)$	9.55 E-3	6.66 E-1	4.29 E-1	4.26 E-1	[illegible] E-1
^{65}Ni	2.6 h	$^{65}Cu(n, p)$	2.69 E-4	1.53 E-1	1.13 E-1	1.91 E-4	[illegible] E-4
Total exposure rate (unshielded): $E = \sum_i E_i$, ΔE according to Eq. (32)				6.53 rem/h	3.22 rem/h	2.[illegible] rem/h	[illegible]
Total personnel exposure rate (shielded): $(E^P \pm \Delta E^P) = 3.45 \cdot 10^{-3} (E \pm \Delta E)$				22.5 mrem/h	11.1 mrem/h	10.0 mrem/h	4.[illegible]

TABLE IV

Preliminary ENDF/B-V Covariance Data (MF=33) Processed with NJOY Code

MAT	Nuclide	MT-Nos. Processed	Reaction Cross Sections
305	B-10	1,2,107,780,781	Total, elastic (n,α), (n,α_0), and (n,α_1)
306	C	1,2,4,51-68,91,102 104,107	Total, elastic, total inelastic, inelastic levels 1-18, inelastic continuum, (n,γ), (n,d), (n,α)
324	Cr	1,2,3,4,16,17,22,28, 102,103,104,105,106, 107	Total, elastic, nonelastic, to-inelastic, (n,2n), (n,3n), (n, n'α), (n,n'p), (n,γ), (n,p), (n,t), (n,d), (n,^{3}He), (n,α)
326	Fe	1,2,3,4,16,22,28,102, 103,104,105,106,107	Total, elastic,nonelastic, total inelastic, (n,2n), (n,n'α), (n,n'p), (n,γ), (n,p), (n,d), (n,t), (n,^{3}He), (n,α)
328	Ni	1,2,4,16,22,28,51-76, 91,102,103 104,107, 111	Total, elastic, total inelastic, (n,2n), (n,n'α), (n,n'p), inelastic levels 1-26, inelastic continuum, (n,γ), (n,p), (n,d), (n,α), (n,2p)
329	Cu	1,2,3,4,16,17,22,28, 102,103,104,106,107	Total, elastic, nonelastic, total inealstic, (n,2n), (n,3n), (n,n'α), (n,n'p), (n,γ), (n,p), (n,d), (n,^{3}He), (n,α)
382	Pb	1,2,3,4,16,17,51,52, 64,102	Total, elastic, nonelastic, total inelastic, (n,2n), (n,3n), inelastic levels 1,2, and 14, (n,α)
1301	Hl	1,2	Total, elastic

TABLE V

Neutron Integral Sensitivity, S_{Σ_T}, of the Inner TF Coil Nuclear Heating Response to the Total Cross Sections of Stainless Steel Components

Component	Region					Total
	6-8	12	14	16	23	
Cr	-0.691	-0.212	-0.[illegible]	-0.150	-0.014	-1.158
Mn	-0.105	-0.034	-0.031	-0.026	-0.005	-0.202
Fe	-2.480	-0.868	-0.767	-0.602	-0.058	-4.775
Ni	-0.526	-0.182	-0.164	-0.140	-0.010	-1.032
Mo	-0.091	-0.033	-0.030	-0.024	-0.008	-0.187
TOTAL	-3.901	-1.330	-1.150	-0.944	-0.097	-7.37[illegible]

TABLE VI

Partial and Net Neutron Integral Sensitivities of the Inner TF Coil Nuclear Heating Response to the Fe Component in Stainless Steel Regions 6-8

Neutron Cross Section, Σ_x	Integral Loss Term	Integral Gain Term	Integral Net, S_{Σ_x}
Σ_a	- 0.17	----	0.17
Σ_s	12.98	10.33	- 2.65
Σ_T	12.81	10.33	- 2.48
$\Sigma_{(n,\gamma)}$	----	0.014	0.014

TABLE VII

Neutron Integral Sensitivity, S_{Σ_T}, of the Inner TF Coil Nuclear Heating Response to the Total Cross Sections of B_4C Components

Component	Region				Total
	11	13	15	17	
10_B	-0.221	-0.[illegible]26	-0.375	-0.5[illegible]3	-1.409
C	-0.166	-0.190	-0.243	-0.196	-0.796
TOTAL	-0.387	-0.459	-0.618	-0.739	-2.[illegible]34

TABLE VIII

Energy-Integrated Relative Sensitivities for NUWMAK

R_1 --- Outer Blanket Breeding Ratio
R_2 --- Outer Blanket Neutron Heating
R_3 --- First Wall Ti dpa Rate
R_4 --- First Wall Ti Gas Production Rate
R_5 --- Neutron Energy Leakage to Inner Magnet
R_6 --- dpa Rate in Al Stabilizer

Cross Section	R_1	R_2	R_3	R_4	R_5	R_6
Ti total	-0.050	-0.079	-0.016	-0.039	-0.349	-0.334
Pb total	0.137	-0.051	0.120	-0.003	-1.598	-1.238
^{12}C total	0.048	-0.024	---	---	-0.633	-0.595
^{10}B total	---	-1.795	---	---	-2.106	-2.094
^{6}Li total	-0.865	-0.652	-0.011	---	-0.025	-0.024
^{7}Li total	-0.011	-0.105	---	0.013	-0.319	-0.303
W total					-5.214	-5.282
Pb(n,2n)	0.115	0.006	0.064	---	-1.078	-0.712
inel. level	0.002	-0.025	-0.024	---	-0.146	-0.154
inel. cont.	-0.022	-0.031	-0.002	---	-0.181	-0.127
elastic	0.040	0.001	0.085	---	-0.181	-0.231
$^{6}Li(n,\alpha)T$	-0.864	-0.644	-0.011	---	-0.001	-0.001
$^{7}Li(n,n'\alpha)T$	-0.036	-0.047	---	-0.007	-0.132	-0.129
elastic	0.023	-0.042	---	0.018	-0.131	-0.119
Ti(n,2n)	0.011	---	0.004	-0.025	-0.097	-0.084
inel. cont.	-0.028	-0.037	-0.017	-0.028	-0.157	-0.152
elastic	0.007	---	0.014	0.018	-0.052	-0.054
W(n,2n)					-4.123	-4.030
inel. cont.					-0.474	-0.622
inel. level					-0.126	-0.143
elastic					-0.451	-0.449

TABLE IX

Relative Uncertainty (%) of the Responses Contributed From the Uncertainties of Total Cross Sections in NUWMAK

Material	$\Delta R/R$ (%)					
	R_i	R_2	R_3	R_4	R_5	R_6
^{6}Li	0.72	0.55	----	0.03	----	----
Pb	0.34	0.10	0.02	0.39	5.02	3.89
^{12}C	0.02	0.02	----	----	1.09	1.78
^{10}B	----	0.39	----	----	----	----
^{7}Li					2.89	2.65
W					42.35	39.86
Ti					2.46	2.14
^{11}B					1.50	1.07
TOTAL $(\sqrt{\Sigma\ \Delta R/R)^2})$	0.80	0.68	0.02	0.39	42.88	40.24

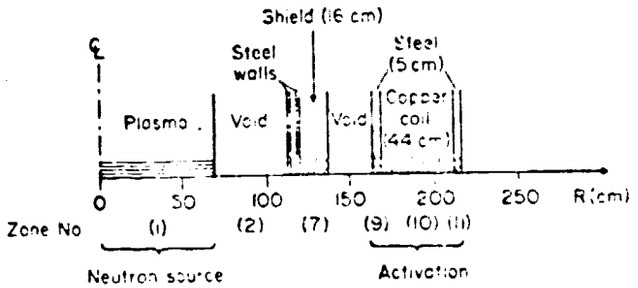

Fig. 1. One-dimensional computational model for TFTR cross-section sensitivity analysis.

Region No.	Region Material	Radius (cm)
		0.0
1	PLASMA	210.0
2	VACUUM	240.0
3	1st WALL S. S.	241.0
4	1st WALL S. S.	242.0
5	1st WALL S. S.	244.0
6	BLANKET S. S.	254.0
7	BLANKET S. S.	264.0
8	BLANKET S. S.	272.0
9	VACUUM	273.0
10	S. S.	276.0
11	B_4C	281.0
12	S. S.	291.0
13	B_4C	297.0
14	S. S.	307.0
15	B_4C	315.0
16	S. S.	325.0
17	B_4C	333.0
18	S. S.	335.0
19	TFC DEWAR S. S.	337.0
20	VACUUM, TUBING, ETC.	339.8
21	THERMAL SHIELD	340.7
22	VACUUM	343.2
23	TFC BOBBIN (S. S.)	345.7
24	TFC	350.7
25	TFC	355.7
26	TFC	360.7
27	TFC	416.2
28	SUPPORT CYLINDER	440.0
29	OHC	465.0

Fig. 2. One-dimensional computational model for EPR inner blanket/shield.

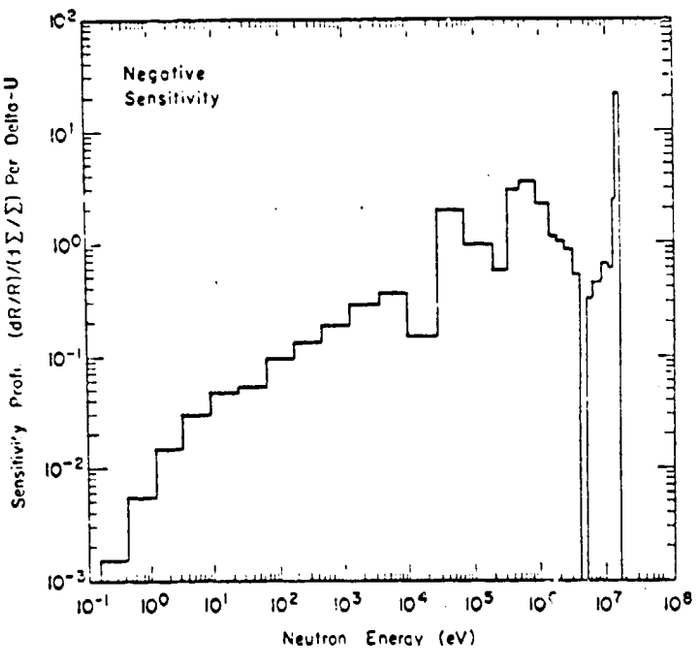

Fig. 3. Sensitivity of the maximum neutron plus gamma-ray heating in the TF coils to all scattering cross sections of Fe.

Fig. 4. SCHEMATIC OF THE BLANKET AND SHIELD FOR NUWMAK

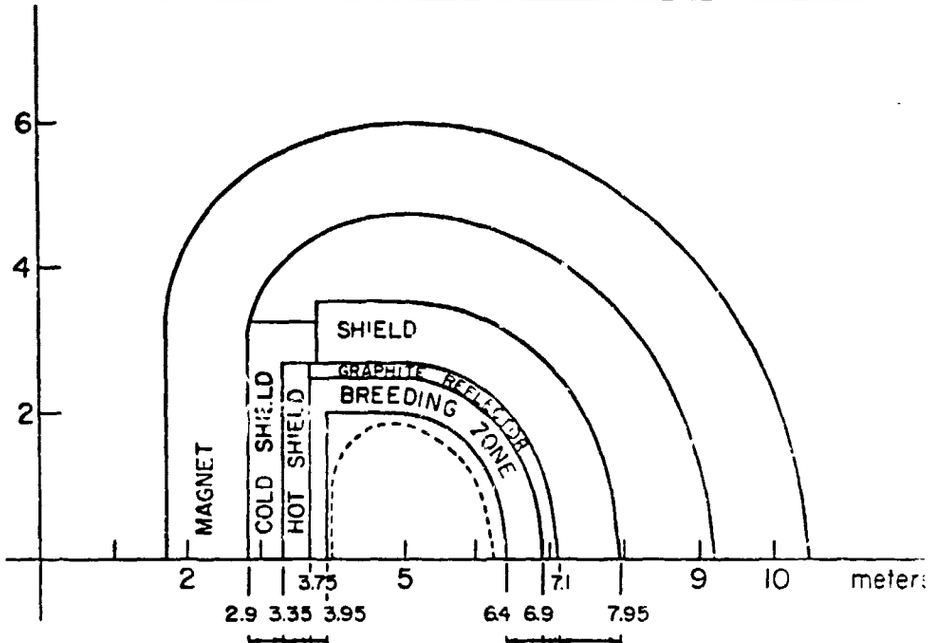

COLD SHIELD	HOT SHIELD	BREEDING ZONE	GRAPHITE REFLECTOR	SHIELD
3.5% Ti alloy	4% Ti alloy	5.7% Ti alloy	3.5% Ti alloy	3.5% Ti alloy
95.25% B_4C	93% W	89.4% Pb Li	95.25% C	95.25% B_4C
1% H_2O	2% H_2O	3.7% H_2O	1% H_2O	1% H_2O
0.25% Pb	1% Pb	1.2% Pb	0.25% Pb	0.25% Pb